DIVERGENT INFLUENCES OF CARDIOVASCULAR DISEASE RISK FACTOR

DOMAINS ON COGNITION, GREY AND WHITE MATTER MORPHOLOGY

[1,2]Mitzi M. Gonzales, Ph.D., [1]Olusola Ajilore, M.D., Ph.D., [3]Rebecca C. Charlton, Ph.D.,

[1]Jamie Cohen, B.A., [1,4,5]Shaolin Yang, Ph.D., [6]Erica Sieg, Psy.D., [1&7]Dulal K. Bhaumik, Ph.D.

[1]Anand Kumar, M.D. & [1]Melissa Lamar, Ph.D.

[1]Department of Psychiatry, University of Illinois at Chicago, Chicago, IL, USA

[2]Department of Mental Health, VA Northern California Healthcare System, Martinez, CA USA

[3]Department of Psychology, Goldsmiths University of London, London, England, UK

[4]Department of Bioengineering, University of Illinois at Chicago, Chicago, IL, USA

[5]Department of Radiology, University of Illinois at Chicago, Chicago, IL, USA

[6]Department of Clinical Psychology, The Chicago School of Professional Psychology, Chicago, IL, USA

[7]Biostatistical Research Center, University of Illinois at Chicago, Chicago, IL, USA

Address for Correspondence: Melissa Lamar, Ph.D.; Rush Alzheimer's Disease Center; 600

South Paulina Street, Room 1029**;** Chicago, IL 60612**;** E-mail: melissa_lamar@rush.edu; Phone:

312-942-3365; Fax: 312-942-2297

Running Title: Cardiovascular Risk and Brain Structure

Word Count 6,500 with references; 4 Tables; 2 Figures

Objective: Hypertension, diabetes, dyslipidemia, and obesity are associated with preclinical alterations in cognition and brain structure; however, this often comes from studies of comprehensive risk scores or single isolated factors. We examined associations of empirically-derived cardiovascular disease risk factor domains with cognition and brain structure.

Methods: 124 adults (age~59.8 ± 13.1;41% African American;50% women) underwent neuropsychological and cardiovascular assessments and structural MRI. Principal component analysis of 9 cardiovascular disease risk factors resulted in a four-component solution representing 1-cholesterol, 2-glucose dysregulation, 3-metabolic dysregulation, and 4-blood pressure. Separate linear regression models for learning, memory, executive functioning and attention/information processing were performed with all components entered at once, adjusting for age, sex, and education. MRI analyses included whole brain cortical thickness and tract-based fractional anisotropy adjusted for age and sex.

Results: Higher blood pressure associated with poorer learning (B=-0.19;p=0.019), memory (B=-0.22;p=0.005), and executive functioning performance (B=-0.14;p=0.031), and lower cortical thickness within the right lateral occipital lobe. Elevated glucose dysregulation associated with poorer attention/information processing performance (B=-0.21;p=0.006) and lower fractional anisotropy in the right inferior and bilateral superior longitudinal fasciculi. Cholesterol was associated with higher cortical thickness within left caudal middle frontal cortex. Metabolic dysfunction was positively associated with right superior parietal lobe, left inferior parietal lobe and left precuneus cortical thickness.

Conclusions: Cardiovascular domains associated with distinct cognitive, grey, and white matter alterations and distinct age groups. Future longitudinal studies may assist in identifying vulnerability profiles that may be most important for individuals with multiple cardiovascular disease risk factors.

Key Words: cardiovascular disease risk factors, blood pressure, glucose, metabolic, cortical thickness, diffusion tensor imaging; white matter integrity

Acronyms: CVD-RF = cardiovascular disease risk factors; BMI = body mass index; DTI = diffusion tensor imaging; FA = fractional anisotropy; HC = healthy controls; SBP = systolic blood pressure; DBP = diastolic blood pressure; Chol = cholesterol; GluDys = glucose dysregulation; MetabDys = metabolic dysregulation; BP = blood pressure; HbA1c = hemoglobin A1c; PCA = principal component analysis; LRN = learning; MEM = memory; EF = executive function; AIP = attention and information processing; CVLT-II = California Verbal Learning Test-II; WMS-III = Wechsler Memory Scales-III; TMT = Trail Making Test; WAIS-III = Wechsler Adult Intelligence Scale-III; GLM = general linear model; FWHM = full width half maximum; QDEC = Query, Design, Estimate, Contrast; TFCE = threshold free cluster enhancement; ILF = inferior longitudinal fasciculus; SLF = superior longitudinal fasciculi

Introduction

Cardiovascular disease risk factors (CVD-RFs) including hypertension, dyslipidemia, diabetes, and obesity increase the likelihood of stroke, heart failure, and mortality (1). CVD-RFs also have a deleterious impact on cognition and brain aging. In fact, all are independent risk factors for cognitive decline and dementia (2,3). Given their frequent comorbidity, CVD-RFs representing distinct pathophysiological processes including hypertension-related reductions in vasodilatory capacity of cerebral arterioles (4) or increases in CNS inflammatory responses secondary to diabetes (5) are often clustered together into a single risk score when investigating brain/behavior relationships (6). These scores have contributed significantly to our understanding that, even in mid-life, higher overall CVD-RF burden is associated with increased risk for dementia in later life (3). While risk scores are advantageous for examining cumulative burden, they present limitations for understanding contributions of distinct CVD-RF domains (7). Advancing our understanding of not only the comorbid impact but also the distinct contributions CVD-RF domains have on brain structure and cognition may assist in identifying 'vulnerability profiles' that may be monitored in affected individuals.

CVD-RF domains may have diverse and potentially antagonistic impact on gray matter morphology. Elevations in systolic and diastolic blood pressure have been associated with diffuse cortical thinning of the frontal, temporal, and occipital lobes, whereas higher cholesterol levels including total and LDL cholesterol and triglycerides have been associated with increased cortical thickness within frontal, temporal, and parietal lobes (8–11). In contrast, glucose dysregulation (as measured by such metrics as fasting glucose, hemoglobin A1c and diabetes diagnosis) and body mass index (BMI) have been weakly and inconsistently related to cortical thickness with results primarily involving frontal, anterior cingulate, temporal, and occipital regions (9–12). These investigations often looked at particular CVD-RFs and/or diagnoses in

isolation (8,11,12), very few took a CVD-RF domain approach to investigate blood pressure, short and longer-term glucose control, 'good' and 'bad' cholesterol, etc. within one study (9,10). Furthermore, given that CVD-RFs predict cognitive decline (2,3) it is unclear how their divergent and often mixed relationship (8–12) with cortical morphology relates to cognition.

CVD-RF domains also have heterogeneous associations with white matter integrity as measured by diffusion tensor imaging (DTI). The most widely used metric of white matter integrity (13) is DTI-derived fractional anisotropy (FA). FA alterations have been extensively linked with CVD-RFs. Individuals with hypertension and diabetes have been shown to have lower FA than controls, with hypertension preferentially affecting posterior brain regions and diabetes impacting more anterior brain regions (14,15). BMI has been positively and negatively associated with regional FA (16,17) as have serum cholesterol levels (18,19). While lower FA has long been associated with cognitive decline in healthy aging (20); fewer studies have explored the role of these CVD-RF-associated FA alterations on cognition. Lower FA has been associated with poorer memory, executive function, and processing speed in both diabetes and untreated hypertension (21,22); further research incorporating more CVD-RF domains is warranted.

Our study aim was to examine the association of multiple CVD-RF domains with cognition and brain structure. We examined the associations of CVD-RF profiles with cognition, grey and white matter in a sample of ethnically diverse, community-dwelling adults. Exploring the relationship of CVD-RFs to cognition in conjunction with grey and white matter integrity may provide insight (23) into the associations of brain/behavior and CVD-RFs (20). We first examined CVD-RFs and cognition, hypothesizing that higher (systolic and diastolic) blood pressure and glucose dysregulation measured using glucose and hemoglobin A1c would be associated with poorer memory, executive function, and attention/information processing. We

then examined associations of CVD-RFs on regional grey and white matter, hypothesizing that higher blood pressure would be associated with lower cortical thickness, whereas higher cholesterol measures would be associated with greater cortical thickness. Furthermore, we hypothesized that elevated blood pressure would be associated with diminished FA in posterior brain regions, whereas increased glucose dysregulation would be associated with lower FA in anterior regions. Finally, we assessed whether CVD-RF related grey and white matter alterations correlated with CVD-RF associated cognitive profiles.

Methods

Participants

Healthy controls (HCs) were identified from a larger program of research investigating aging, diabetes and depression approved by the University of Illinois at Chicago Institutional Review board and conducted in accordance with the Declaration of Helsinki. HCs provided written informed consent at enrollment. As previously described (6), HCs, aged 30 years and older (range=30-89), were recruited from the community between 10/2009-08/2012 and underwent an initial telephone screening to rule-out neurological and/or Axis 1 disorders, head injury or loss of consciousness, substance abuse/dependence, and/or psychotropic medication use. Upon successful completion of the telephone screen, study staff including board eligible/certified psychiatrists conducted a more detailed in person screening. HC status was confirmed if: 1) Mini-Mental State Examination (24) scores were $\geq$24, 2) there was an absence of current and/or past psychiatric symptoms as assessed by the Structured Clinical Interview for DSM-IV and 3) Hamilton Depression Rating Scale scores were <8.

Of 124 eligible participants (Table 1), 43 (34.7%) met criteria for diabetes (non-fasting glucose$\geq$200 mg/dl or anti-diabetic mediation use) (25), a rate higher than the Illinois state average (23.8%) (26) and likely attributable to active recruitment of individuals with diabetes in

the larger research. Seventy participants were hypertensive (systolic blood pressure [SBP]$\geq$140 mmHg, diastolic blood pressure [DBP]$\geq$90 mmHg, or antihypertensive medication use) (27), 54 met criteria for obesity (BMI$\geq$30 kg/m^2) (28), 40 had hypercholesterolemia (total cholesterol$\geq$240 mg/dl or lipid lowering medication use) (29), and 27 did not met criteria for any of these conditions. Forty-two participants were on anti-diabetic medications, 50 were on antihypertensives, and 36 were on lipid lowering medications.

CVD-RF Assessment

One reading of brachial SBP and DBP were obtained with the participant sitting upright using an automated device (Welch Allyn, model 300, Welch Allyn Inc., Arden, NC) and appropriate cuff size. Weight in kilograms and height in centimeters were collected to calculate BMI. A non-fasting blood sample was obtained by venipuncture to determine plasma concentrations of glucose, total cholesterol, HDL-cholesterol, LDL-cholesterol, triglycerides, and hemoglobin A1c (HbA1c). Cholesterol and HbA1c values have been documented to be minimally affected by normal food consumption (30).

In order to allow for the consideration of CVD-RF domains without treating any one CVD-RF in isolation at the expense of another, we took our lead from the literature on studies of biological determinants of cerebrovascular health (8,9). As suggested by the literature (8,9), CVD-RF metrics of interest (SBP, DBP, BMI, glucose, total cholesterol, inverted HDL-cholesterol, LDL-cholesterol, triglycerides, and HbA1c) were submitted to a PCA with varimax rotation to empirically determine the CVD-RF metrics that had high shared variance (e.g., SBP and DBP; glucose and HbA1c) and to control for multiple comparisons.

Similar to previous research using this technique (8,9), our PCA resulted in four orthogonal factors that explained 78.0% variance (minimum eigenvalue=1; Table 2) representing Cholesterol (Chol; Component #1), Glucose Dysregulation (GluDys; Component #2), Metabolic

Dysregulation (MetabDys; Component #3), and Blood Pressure (BP; Component #4). While consistent with prior research (9), our MetabDsy loadings were more robust, likely due to the omission of previously documented (9) low-loading creatine from our analyses. PCA marker variables guided the creation of domain scores to represent CVD-RFs with the highest shared variance per Component (e.g., Component 4: SBP and DBP; Component 2: glucose and HbA1c) (31). Raw scores for the highest loadings per Component (Table 2) were transformed into standardized z-scores based on the study sample's mean and standard deviation and averaged to create BP, GluDys, MetabDys, and Chol domain scores.

Neuropsychological Assessment

Conducted by a trained research assistant and described in detail elsewhere (6), cognitive domains were calculated by averaging z-scores within each construct tested: (1) Learning (LRN): immediate recall from the California Verbal Learning Test-II (CVLT-II) Trials 1-5 (32) and the Wechsler Memory Scales-III (WMS-III) Logical Memory-I and Visual Reproduction-I (33); (2) Memory (MEM): CVLT-II long delay free recall (32), WMS-III Logical Memory-II and Visual Reproduction-II (33); (3) Executive Function (EF): Trail Making Test (TMT) Part B time to completion (34) (reversed), Delis-Kaplan Executive Function System category switching total (35), Stroop Interference score (36), Wechsler Adult Intelligence Scale-III (WAIS-III) Digit Span Backwards raw score (37), Self-Ordered Pointing Task total errors (38) (reversed); (4) Attention and Information Processing (AIP): TMT Part A time to completion (34) (reversed), Stroop Color and Word raw scores (36), WAIS-III Digit-Symbol Coding raw score (37). Cronbach's alphas revealed adequate internal consistency (LRN=0.75, MEM=0.75, EF=0.73, AIP=0.84).

MRI Acquisition

Whole brain MRI data in the axial plane were collected on a Philips Achieva 3T scanner (Philips Medical Systems, the Netherlands) using an 8-channel sensitivity encoding head coil. Anatomical image data were collected using MPRAGE (FOV=240mm, contiguous slices=134, TR/TE=8.4/3.9ms, flip angle=8°, voxel size=$1.1\times1.1\times1.1$mm^3). DTI was obtained aligned to the anterior commissure-posterior commissure line, using a single-shot spin-echo echo-planar imaging sequence (FOV=240mm, contiguous slices=67, TR/TE=6,994/71ms, flip angle=90°, voxel size=$0.83\times0.83\times2.2$mm^3, 32 isotropically distributed diffusion-weighted directions with b=700s/mm^2, and one B$_0$ images with no diffusion sensitization). Scanning time was reduced to ~4 minutes using a SENSE parallel imaging technique with a factor of 2.5.

Of the 124 subjects with available cognitive and cardiovascular data, 86 had T$_1$ images. Reasons for unavailable T$_1$ data included: claustrophobia=11; BMI=4; metallic implants=3; scanner problems=19; poor image quality=1. Twenty-four did not complete DTI due to time constraints and another 9 were removed for poor quality images (DTI n=53). Individuals with available MRI data were older than those without MRI data (61.7 ± 12.6 versus 55.6 ± 13.2; p=.017); groups did not differ in education or sex.

Image Processing

All MRI data was visually examined for quality. This inspection included an examination for artifacts from movement or other causes, such as space-occupying or other focal lesions, including stroke and other gross neuroanatomical abnormalities. As outlined above, 10 participants were excluded based on this inspection.

Cortical thickness quantification was conducted in FreeSurfer Version 5.3.0 (http://surfer.nmr.mgh.harvard.edu/). Following motion correction and skull stripping, thickness measurements were derived at each vertex along the reconstructed surface by computing the

shortest distance between the outer cortical (pial) surface and grey/white matter border (39,40). These measurements were mapped onto each participant's inflated cortical surface and checked for quality control by viewing individual images in tkmedit and tksurfer. A spherical averaging procedure was implemented to average thickness measurements across participants.

DTI analysis, implemented in FSL v4.1.9 (http:/www.fmrib.ox.ac.uk/fsl), used FMRIB's Diffusion Toolbox and Tract-Based Spatial Statistics (41). FA images underwent motion correction and skull stripping, normalization to the $1mm^3$ MNI152 stereotaxic space by implementing a nonlinear registration of each participant's FA image to the FSL FA template and then applying an affine transformation to the MN1152 template – images were then visually inspected for errors in processing and/or distortion. Normalized FA images were averaged to create a mean FA map. A mean FA skeleton was derived by applying a 0.2 threshold (41) and images were then visually inspected to ensure that the major tracts were well aligned to the skeleton. Each participant's FA data was projected onto the group skeleton to identify the highest local FA value and then applied to the skeleton.

Statistical Analysis

Associations between CVD-RF and cognition domains were assessed using IBM SPSS Statistics 22 (IBM Corp, Armonk, NY). Separate linear regression models ($p \leq 0.05$) assessed each cognitive domain score individually (4 models) with all CVD-RF domain scores entered at once, adjusting for age, sex, and education. Additional adjustments for race, smoking status (current smoker: yes/no) and treatment effects (presence/absence of medication use for hypertension, diabetes and/or hypercholesterolemia) were also considered. Given the age range of our sample (30-89 years), we explored age as a moderator variable by adding an interaction term between significant CVD-RF domains and age as appropriate.

The relationship between individual CVD-RF domains and cortical thickness was evaluated using a general linear model (GLM) at each vertex in the cortical mantle adjusting for age and sex using the Query, Design, Estimate, Contrast (QDEC) interface in FreeSurfer (www.surfer.nmr.mgh.harvard.edu; 42). Maps were smoothed with a 15mm full width half maximum (FWHM) Gaussian kernel, a more conservative threshold than prior relevant studies (9,10). Correction for multiple comparisons was performed with a cluster-wise procedure using Monte Carlo Null-z simulation method within the QDEC processing stream (43). For each model, 10,000 iterations of the stimulation were performed using a threshold of 1.3 ($p<0.05$). Mean cortical thickness in identified clusters was extracted within QDEC. In supplementary regression analyses, associations between individual regions of interest (ROIs) derived from the FreeSurfer atlas and CVD-RF domains as well as individual CVD-RF variables were assessed adjusting for age and sex.

Associations between CVD-RF domains and FA, adjusting for age and sex, were assessed using regression models adjusted for age and sex. Five thousand permutations were performed and cluster-based thresholding correction was implemented with threshold free cluster enhancement (TFCE) (44). Statistical maps were then thresholded at $p<0.001$ and clusters sizes larger than 100 voxels were identified. The anatomical location of significant clusters was identified using JHU ICBM-DTI-81 White Matter Labels and JHU White Matter Tractography (45) and mean FA values were extracted using FSL.

Due to the truncated MRI sample, we examined the association between CVD-RF related morphological alterations, cortical thickness and FA clusters significantly associated with CVD-RFs, defined and extracted as described above, with their respective CVD-RF cognitive associates using two-sided Pearson's correlations ($p\leq0.05$) in SPSS. We also ran more stringent

mediation (46) and indirect mediation analyses with bootstrapping using Preacher and Hayes methods (47,48).

Results

Cognition– In separate cognitive models with all cardiovascular domains (BP, GluDys, Chol and MetabDys) entered simultaneously adjusting for age, sex and education, only BP domain scores were significantly and negatively associated with LRN (B=-0.19,SE=0.08;p=0.019) and MEM (B=-0.22,SE=0.07;p=0.005) performance. In contrast, BP as well as GluDys domain scores negatively associated with EF (BP: B=-0.14,SE=0.06;p=0.031; GluDys: B=-0.11,SE=0.06;p=0.058); however, only the BP domain score reached significance (Table 3). Only GluDys domain scores significantly and negatively associated with poorer AIP (B=-0.21,SE=0.07;p=0.006). No associations were observed for Chol or MetabDys. Results remained unchanged with further adjustments for race, smoking status and treatment effects except the BP and EF association was no longer significant.

Exploring age as a moderator variable resulted in a significant age X BP interaction for LRN (p=0.027) and MEM (p=0.014) only; there were no significant age x GluDys interactions (all p-values≥0.65). After adjusting for all covariates including race, smoking status and treatment effects, only the age X BP interaction for MEM remained significant (p=0.048). A follow-up Johnson-Neyman plot revealed a cut-point of significance occurring for the conditional effect of BP on MEM such that individuals <64.4 years old showed a significant association between BP and MEM (all p-values≤0.050) while individuals ≥64.4 years of age did not (all p-values≥0.072).

Cortical Thickness– Higher BP domain scores were associated with lower cortical thickness in the right lateral occipital lobe controlling for age and sex (Figure 1a). No significant associations between cortical thickness and GluDys were observed (Table 4). Chol domain scores positively

associated with cortical thickness within the left caudal medial frontal cortex after adjustment for age and sex (Figure 1b). Higher MetabDys domain scores were associated with higher cortical thickness measures in the right superior parietal lobe, left inferior parietal lobe, and left precuneus after adjustments for age and sex (Figure 1b). Additional adjustments for race, smoking status and treatment effects did not alter these results. For completeness, FreeSurfer cortical thickness ROIs as analyzed individually is represented in Supplemental Table I with regressions between individual CVD-RFs that comprised each domain score and results of these individual analyses shown in Supplemental Table II.

An initially significant age X BP interaction for the right lateral occipital lobe adjusting for age and sex (p<0.001) did not remain significant after adding race, smoking status and treatment effects to the model (p=0.791). Exploring age as a moderator variable did not reveal any significant age X Chol or age X MetabDys interactions regardless of adjustments (all p-values≥0.110).

DTI tractography–After adjustment for age and sex, higher GluDys domain scores associated with lower FA in the right inferior longitudinal fasciculus (ILF) and bilateral superior longitudinal fasciculi (SLF; Figure 2). No other CVD-RF domain scores associated with FA in models adjusted for age and sex. Additional adjustments for race, smoking status and treatment effects did not alter our results.

Exploring age as a moderator variable revealed significant age X GluDys interactions for all identified white matter tracts listed when only age and sex were in the model (all p-values≥0.044). Only the age X GluDys interaction in the right SLF model remained significant after adding race, smoking status and treatment effects to the model (p=0.001). Johnson-Neyman plots revealed a cut-point of significance occurring for the conditional effect of GluDys on right SLF FA with individuals <56.4 years of age showing a significant association between GluDys

and FA in the right SLF (all p-values≤0.050) and individuals ≥56.4 years of age not showing this association.

Neuroimaging and Cognition–We extracted the cortical thickness and FA cluster measures associated with CVD-RF domain scores to determine whether these clusters significantly correlated with their relevant CVD-RF cognitive associates. For example, LRN, MEM and EF correlates to BP were subjected to two-tailed Pearson's correlations with the lateral occipital cortical thickness cluster (also associated with BP); no cognitive domains correlated with this thickness measure. When considering the white matter tracts significantly correlated with GluDys, EF (a trending correlation with GluDys) was positively associated with right ILF FA values [r(df=51)=0.30,p=0.027] and bilateral SLF values [left: r(df=51)=0.32,p=0.020; right: r(df=51)=0.33,p=0.014] while AIP scores significantly related to GluDys positively correlated with right SLF FA values [r(df=51)=0.27,p=0.048]. Indirect mediation analyses with bootstrapping did not corroborate these results, i.e., no mediation or indirect pathway results were significant.

Discussion

The overarching message from this research is that CVD-RF domains had more divergent than convergent influences on cognition and brain structure. For example, BP and GluDys domains were more strongly associated with cognition than Chol and MetabDys domains. Additionally, BP, Chol and MetabDys were associated with cortical thickness either negatively (BP) or positively (Chol and MetabDys), while only GluDys related to (lower) FA. Similarly, only GluDys-related FA alterations associated with poorer cognitive functioning suggesting this was the most consistent of our brain/behavior relationship findings. While these results may highlight the unique information derived by the examination of empirically derived CVD-RF domains, when combined with our results using age as a moderator variable, this study highlights the

importance of considering how age may influence brain/behavior associates of CVD-RFs – an area of increased interest across multiple CVD-RFs (49–51).

Only BP and GluDys emerged as salient associates of cognition. Specifically, higher BP associated with poorer LRN, MEM, and EF while greater GluDys associated with poorer AIP and poorer EF (albeit a non-significant trend). These findings are consistent with a systematic review of the literature that showed hypertension and diabetes display a consistent detrimental impact on cognition whereas obesity and dyslipidemia have weak and variable effects (52). This may be due to the age of participants across studies, i.e., mid- versus late-life (52), and/or the grouping of obesity and dyslipidemia – variables increasingly seen to be distinct (8). Our results also indicate that continuous blood pressure and glucose measurements are negatively associated with cognition regardless of a diagnosis of hypertension and/or diabetes. Given that continuous measures incorporate pre-clinical levels of disease known to be detrimental to brain health (17,53), our results may be early support for such recent recommendations as lowing the 'optimal' SBP to <120mmHg (54). While further research is needed to fully determine the inflection points beyond which cognition is negatively impacted by BP or glucose, this study and others (55) suggest focusing on particular age ranges, e.g., individuals less than age 65 when considering BP, may facilitate this work.

Cardiovascular domains had distinct and competing influences on cortical thickness. Higher BP related to lower cortical thickness in posterior regions, while higher Chol was related to greater cortical thickness in more anterior regions. Higher MetabDys also associated with greater cortical thickness, however, in more posterior, e.g., parietal regions. While cholesterol and metabolic-related results regarding cortical thickness may not be intuitive, other studies report similar findings (8,9,56). In fact, these studies advocate that BMI and lipids may not be consistently related to each other but instead, may be independent CVD-RFs (8), they may also

require a non-linear approach to understanding their brain-behavior relationships. Additionally, grey matter measures vary in the literature, introducing differences between cortical thickness and grey matter volume that may influence CVD-RF associations, e.g., cortical thickness is more vulnerable to environmental exposures while both measures have distinct genetic influences. Genetic factors link cholesterol levels in the peripheral and central nervous systems; this may differentially impact associations made between genetic regulation of circulating cholesterol and alterations in grey as well as white matter morphology (18) further influencing our results.

Elevations in BP were negatively associated with cortical thickness in the lateral occipital cortex, in line with studies demonstrating that hypertension induces cortical degradation in posterior regions including the parietal and occipital lobe, areas typically preserved in healthy aging (15). This may be due, in part, to the fact that BP elevations can diminish blood brain barrier integrity, which disrupts nutrient delivery and propagates neuronal damage, potentially resulting in cortical thinning (53,57). Furthermore, chronic elevations in BP can reduce the vasodilatory capacity of the cerebral arterioles by increasing media thickness and narrowing the lumen (58). Subsequent reductions in cerebral blood flow may result in hypoperfusion and induce neuronal damage and grey matter atrophy (42).

GluDys was the only factor associated with TBSS-derived FA values and FA subsequently correlated with the cognitive domains shown to be related to GluDys; the only white matter findings related to CVD-RFs and their relevant CVD-RF cognitive associates. Some GluDys-related white matter associates were driven by younger participants, thus, the wide 30-89 age range of our sample may have precluded replication of previously reported BP and FA associations (15). In contrast, and consistent with other studies (14,17), higher GluDys was associated with lower FA in the right ILF and SLF, bilaterally – key white matter tracts connecting posterior to more anterior regions of brain to facilitate higher-level cognitive

functions. Elevations in glucose dysregulation may impact FA by propagating pro-inflammatory cytokines (59) capable of crossing the blood brain barrier (60), and instigating a local CNS inflammatory response characterized by activation of microglial cells (61). Activated microglia, in turn, may impede the development and migration of oligodendrocyte progenitor cells (62), disrupting myelin production and diminishing white matter integrity as well as the successful relay of information to perform executive functioning and attention/information processing tasks. Future work focusing on the role of CVD-RFs, particularly glucose, on myelin degradation may assist in determining the underlying etiology of our findings (63).

While this study examined a broad range of cardiovascular, cognitive, and brain morphology factors, limitations exist. Consistent with prior literature (8,9), we utilized PCA to create CVD-RF domains consisting of factors with high shared variance. While this approach is efficacious for creating empirically defined groups of highly similar variables, reducing redundancy, and diminishing multiple comparisons, BMI loaded onto both the GluDys and MetabDys domains – albeit with lower values than any other variable loading in the PCA. This may suggest that BMI is either a multidimensional variable and/or one that did not exert as strong a contribution as other CVD-RFs in our PCA. Future studies should incorporate more direct assessments of adiposity such as those provided by dual-energy x-ray absorptiometry scanning. Our cross-sectional design precludes determination of causation, making longitudinal studies necessary. Additionally, larger sample sizes will be necessary to empirically examine the interplay between cortical thickness and white matter alterations (23). The neuroimaging and cognition mediation analyses and assessment of indirect effects may have suffered from a truncated neuroimaging sample making our call for larger sample sizes even more germane. These analyses may also have suffered from a limited number of cognitive domains, i.e., a

visuospatial/visuoperceptual component may have related to BP and its lateral occipital associates.

DTI-derived FA reflects diverse morphological changes such as alterations in myelination, axonal density, inflammation, and edema (13). While FA may be divided into axial and radial diffusivity, many argue that these measures are not only influenced by inflammation and edema, they are highly correlated and may not reflect axonal loss (i.e., axial diffusivity) and myelin degradation (i.e., radial diffusivity) in isolation (13,63,64). Neuroimaging techniques including multi-component relaxometry (64), which eliminate the influence of inflammation and edema, may provide greater insight into underlying etiological factors driving white matter associates to CVD-RFs including white matter perfusion and demyelination (63). Future studies should compare the various microstructural metrics for axonal loss and myelin degradation both to each other as well as to CVD-RF profiles to better understand the underlying neuroanatomy driving the results of this study. Contrary to previous studies (15), elevations in BP were not related to FA. This may be due, in part, to the fact that we only obtained one BP recording as opposed to the recommended minimum of two (65) that would have reduced variability inherent in a single measurement. Having said that, previous studies show that early elevations in BP may impact the cortical mantle with white matter damage emerging later as chronic hypoperfusion ensues (53); unfortunately we did not have the sample size to divide our group by age-decades to investigate this possibility. Finally, although cluster-based thresholding procedures to adjust for multiple comparisons are standard in the literature, these procedures may still result in an inflated Type-I error (66).

Similar to their impact on the peripheral nervous system (67), CVD-RFs may induce perturbations across multiple physiological pathways, resulting in distinct yet phenotypic brain alterations that may ultimately contribute to pathological aging and dementia. Given that CVD-

RFs are modifiable, and optimal control recommendations continue to gravitate toward a more conservative approach (54), understanding their distinct and overlapping associations on brain aging in early, mid-, and late-life as distinct time periods may help highlight the beneficial effects of lowering levels of cardiovascular risk at particular points across the lifespan.

References

1. Lloyd-Jones D, Adams RJ, Brown TM, Carnethon M, Dai S, De Simone G, Ferguson TB, Ford E, Furie K, Gillespie C, Go A, Greenlund K, Haase N, Hailpern S, Ho M, Howard V, Kissela B, Kittner S, Lackland D, Lisabeth L, Marelli A, McDermott MM, Meigs J, Mozaffarian D, Mussolino M, Nichol G, Roger VL, Rosamond W, Sacco R, Sorlie P, Stafford R, Thom T, Wasserthiel-Smoller S, Wong ND, Wylie-Rosett J. Heart disease and stroke statistics-2010 update: a report from the American Heart Association. Circulation 2010;121:46–215.

2. Elias MF, Elias PK, Sullivan LM, Wolf PA, D'Agostino RB. Obesity, diabetes and cognitive deficit: the Framingham Heart Study. Neurobiol Aging 2005;26:11–6.

3. Whitmer RA, Sidney S, Selby J, Johnston SC, Yaffe K. Midlife cardiovascular risk factors and risk of dementia in late life. Neurology 2005;64:277–81.

4. Beason-Held LL, Moghekar A, Zonderman AB, Kraut MA, Resnick SM. Longitudinal Changes in Cerebral Blood Flow in the Older Hypertensive Brain. Stroke 2007; 38:1766–73.

5. Kim E, Tolhurst AT, Cho S. Deregulation of inflammatory response in the diabetic condition is associated with increased ischemic brain injury. J Neuroinflammation 2014;11:83.

6. Lamar M, Rubin L, Ajilore O, Zhang A, Yang S, Cohen J, Kumar A. Risk & diagnosis of diabetes: What metabolic syndrome contributes to brain outcomes in African American and Caucasian cohorts. Curr Alzheimer's Res 2015;12:640–7.

7. Oda E. Metabolic syndrome: its history, mechanisms, and limitations. Acta Diabetol 2012;49:89–95.

8. Krishnadas R, McLean J, Batty DG, Burns H, Deans KA, Ford I, McConnachie A, McGinty A, McLean JS, Millar K, Sattar N, Shiels PG, Velupillai, Packard CJ, Cavanagh J. Cardio-metabolic risk factors and cortical thickness in a neurologically healthy male population: results from the psychological, social and biological determinants of ill health (pSoBid) study. NeuroImage Clin 2013;2:646–57.

9. Leritz EC, Salat DH, Williams VJ, Schnyer DM, Rudolph JL, Lipsitz L, Lischl B, McGlinchey RE, Milberg WP. Thickness of the human cerebral cortex is associated with metrics of cerebrovascular health in a normative sample of community dwelling older adults. NeuroImage 2011;54:2659–71.

10. Vuorinen M, Kareholt I, Julkunen V, Spulber G, Niskanen E, Paajanen T, Soininen H, Kivipelto M, Solomon A. Changes in vascular factors 28 years from midlife and late-life cortical thickness. Neurobiol Aging 2013;34:100–9.

11. Seo SW, Lee JM, Im K, Park JS, Kim SH, Kim ST, Ahn AJ, Kim MJ, Kim GH, Kim JH, Roh JH, Cheong HK, Na DL. Cardiovascular risk factors cause cortical thinning in cognitively impaired patients: relationships among cardiovascular risk factors, white matter hyperintensities, and cortical atrophy. Alzheimer Dis Assoc Disord 2012;26:106–12.

12. Ajilore O, Narr K, Rosenthal J, Pham D, Hamilton L, Watari K, Elderkin-Thompson V, Darwin C, Toga A, Kumar A. Regional cortical gray matter thickness differences

associated with type 2 diabetes and major depression. Psychiatry Res Neuroimaging 2010;184:63–70.

13. Beaulieu C. The basis of anisotropic water diffusion in the nervous system–a technical review. NMR Biomed 2002;15:435–55.

14. H Hsu J JL, Chen YL, Leu JG, Jaw FS, Lee CH, Tsai YF, Hsu CY, Bai CH, Leemans A. Microstructural white matter abnormalities in type 2 diabetes mellitus: a diffusion tensor imaging study. NeuroImage 2012;59:1098–105.

15. Kennedy KM, Raz N. Pattern of normal age-related regional differences in white matter microstructure is modified by vascular risk. Brain Res 2009;1297:41–56.

16. Verstynen TD, Weinstein AM, Schneider WW, Jakicic JM, Rofey DL, Erickson KI. Increased body mass index is associated with a global and distributed decrease in white matter microstructural integrity. Psychosom Med 2012;74:682–90.

17. Verstynen TD, Weinstein A, Erickson KI, Sheu LK, Marsland AL, Gianaros PJ. Competing physiological pathways link individual differences in weight and abdominal adiposity to white matter microstructure. NeuroImage 2013;79:129–37.

18. Warstadt NM, Dennis EL, Jahanshad N, Kohannim O, Nir TM, McMahon KL, de Zubicaray GI, Montgomery GW, Henders AK, Martin NG, Whitfield JB, Jack CR, Bernstein MA, Weiner MW, Toga AW, Wright MJ, Thompson PM, Alzheimer's Disease Neuroimaging Initiative (ADNI). Serum cholesterol and variant in cholesterol-related gene CETP predict white matter microstructure. Neurobiol Aging 2014;35:2504–13.

19. Williams VJ, Leritz EC, Shepel J, McGlinchey RE, Milberg WP, Rudolph JL, Lipsitz LA, Salat DH. Interindividual variation in serum cholesterol is associated with regional white matter tissue integrity in older adults. Hum Brain Mapp 2013;34:1826–41.

20. Ziegler DA, Piguet O, Salat DH, Prince K, Connally E, Corkin S. Cognition in healthy aging is related to regional white matter integrity, but not cortical thickness. Neurobiol Aging 2010;31:1912–26.

21. Hannesdottir K, Nitkunan A, Charlton RA, Barrick TR, MacGregor GA, Markus HS. Cognitive impairment and white matter damage in hypertension: a pilot study. Acta Neurol Scand 2009;119:261–8.

22. Reijmer YD, Brundel M, de Bresser J, Kappelle LJ, Leemans A, Biessels GJ. Microstructural white matter abnormalities and cognitive functioning in type 2 diabetes A diffusion tensor imaging study. Diabetes Care 2013;36:137–44.

23. Tuladhar AM, Reid AT, Shumskaya E, Laat KF de, Norden AGW van, Dijk EJ van, Norris DG, de Leeuw FE. Relationship between white matter hyperintensities, cortical thickness, and cognition. Stroke 2015;46:425–32.

24. Folstein MF, Folstein SE, P. R McHugh. Mini-Mental State: a practical method for grading the cognitive state of patients for the clinician. J Psychiatr Res 1975;12:189–98.

25. American Diabetes Association. Diagnosis and classification of Diabetes Mellitus. Diabetes Care 2010;33:S62–9.

26. Danaei G, Friedman AB, Oza S, Murray CJ, Ezzati M. Diabetes prevalence and diagnosis in US states: analysis of health surveys. Popul Health Metr 2009;7:16.

27. Fagard RH, Van den Enden M, Leeman M, Warling X. Survey on treatment of hypertension and implementation of World Health Organization/International Society of Hypertension risk stratification in primary care in Belgium. J Hypertens 2002;20:1297–302.

28. World Health Organization. Obesity: preventing and managing the global epidemic. Report of a WHO consultation. Geneva, Switzerland: World Health Organization; 2000.

29. Expert Panel on Detection, Evaluation, and Treatment of High Blood Cholesterol in Adults. Executive summary of the third report of the national cholesterol education program (ncep) expert panel on detection, evaluation, and treatment of high blood cholesterol in adults (adult treatment panel iii). JAMA 2001;285:2486–97.

30. Langsted A, Freiberg JJ, Nordestgaard BG. Fasting and nonfasting lipid levels influence of normal food intake on lipids, lipoproteins, apolipoproteins, and cardiovascular risk prediction. Circulation 2008;118:2047–56.

31. DiStefano C, Zhu M, Mindrila D. Understanding and using factor scores: Considerations for the applied researcher. Pract Assess Res Eval 2009;14:1–11.

32. Delis D, Kaplan E, Kramer JH, Ober BA. California Verbal Learning Test-II. San Antonio: The Psychological Corporation; 2000.

33. Wechsler D. Wechsler Memory Scale. Third ed. San Antonio: Psychological Corporation; 1997.

34. Reitan RM. Validity of the Trail Making Test as an indicator of organic brain damage. Percept Mot Skills 1958;8:271–6.

35. Delis DC, Kaplan E, Kramer JH. Delis-Kaplan Executive Function System (D-KEFS). San Antonio: Psychological Corporation; 2001.

36. Golden CJ. S Stroop Color and Word Test: A Manual for Clinical and Experimental Uses. Chicago: Skoelting; 1978.

37. Wechsler D. Administration and scoring manual for the Wechsler Adult Intelligence Scale. Third ed. San Antonio: The Psychological Corporation; 1997.

38. Petrides M, Alivisatos B, Frey S. Differential activation of the human orbital, mid-ventrolateral, and mid-dorsolateral prefrontal cortex during the processing of visual stimuli. Proc Natl Acad Sci 2002;99:5649–54.

39. Dale AM, Fischl B, Sereno MI. Cortical surface-based analysis: I. Segmentation and surface reconstruction. NeuroImage 1999;9:179–94.

40. Fischl B, Dale AM. Measuring the thickness of the human cerebral cortex from magnetic resonance images. Proc Natl Acad Sci 2000;97:11050–55.

41. Smith SM, Jenkinson M, Johansen-Berg H, Rueckert D, Nichols TE, Mackay CE, Watkins KE, Ciccarelli O, Cader MZ, Matthews PM. Tract-based spatial statistics: voxelwise analysis of multi-subject diffusion data. NeuroImage.2006;31:1487–505.

42. Hagler DJ, Saygin AP, Sereno MI. Smoothing and cluster thresholding for cortical surface-based group analysis of fMRI data. NeuroImage 2006;33:1093–103.

43. Lindquist MA, Mejia A. Zen and the art of multiple comparisons. Psychosom Med 2015;77:114–25.

44. Smith SM, Nichols TE. Threshold-free cluster enhancement: addressing problems of smoothing, threshold dependence and localisation in cluster inference. NeuroImage 2009;44:83–98.

45. Mori S, Oishi K, Faria AV. White matter atlases based on diffusion tensor imaging. Curr Opin Neurol 2009;22:362–9.

46. Muller D, Judd CM, Yzerbyt VY. When moderation is mediated and mediation is moderated. J Pers Soc Psychol 2005;89:852-63.

47. Preacher KJ, Hayes AF. SPSS and SAS procedures for estimating indirect effects in simple mediation models. Behav Res Methods Instrum Comput 2004;36:717–31.

48. Hayes AF. Beyond Baron and Kenny: Statistical mediation analysis in the new millennium. Commun Monogr 2009;76:408–20.

49. Ryan JP, Aizenstein HJ, Orchard TJ, Ryan CM, Saxton JA, Fine DF, Nunley KA, Rosano C. Age of childhood onset in Type 1 Diabetes and functional brain connectivity in midlife. Psychosom Med 2015;77:622–30.

50. Bischof GN, Park DC. Obesity and aging: consequences for cognition, brain structure, and brain function. Psychosom Med 2015;77:697–709.

51. Seaquist ER. The impact of diabetes on cerebral structure and gunction. Psychosom Med. 2015;77:616–21.

52. Van Den Berg E, Kloppenborg RP, Kessels RP, Kappelle LJ, Biessels GJ. Type 2 diabetes mellitus, hypertension, dyslipidemia and obesity: A systematic comparison of their impact on cognition. Biochim Biophys Acta BBA-Mol Basis Dis 2009;1792:470–81.

53. Gianaros PJ, Greer PJ, Ryan CM, Jennings JR. Higher blood pressure predicts lower regional grey matter volume: Consequences on short-term information processing. NeuroImage 2006;31:754–65.

54. National Heart, Lung, and Blood Institute. Landmark NIH study shows intensive blood pressure management may save lives. National Institutes of Health [Internet]. US Department of Health and Human Services; 2015; Available from: http://www.nih.gov/news/health/sep2015/nhlbi-11.htm

55. Gottesman RF, Schneider ALC, Albert M, Alonso A, Bandeen-Roche K, Coker L, Coresh J, Knopman D, Power MC, Rawlings A. Midlife hypertension and 20-year cognitive change: the atherosclerosis risk in communities neurocognitive study. JAMA Neurol 2014;71:1218–27.

56. Kaur S, Gonzales MM, Strasser B, Pasha E, McNeely J, Tanaka H, Haley AP. Central adiposity and cortical thickness in midlife. Psychosom Med 2015;77:671–78.

57. Al-Sarraf H, Philip L. Effect of hypertension on the integrity of blood brain and blood CSF barriers, cerebral blood flow and CSF secretion in the rat. Brain Res 2003;975:179–88.

58. Heistad DD, Baumbach GL. Cerebral vascular changes during chronic hypertension: good guys and bad guys. J Hypertens 1992;10:S71-75.

59. Shanmugam N, Reddy MA, Guha M, Natarajan R. High glucose-induced expression of proinflammatory cytokine and chemokine genes in monocytic cells. Diabetes 2003;52:1256–64.

60. Ek M, Engblom D, Saha S, Blomqvist A, Jakobsson P-J, Ericsson-Dahlstrand A. Inflammatory response: pathway across the blood–brain barrier. Nature 2001;410:430–1.

61. Ponomarev ED, Maresz K, Tan Y, Dittel BN. CNS-derived interleukin-4 is essential for the regulation of autoimmune inflammation and induces a state of alternative activation in microglial cells. J Neurosci 2007;27:10714–21.

62. Simpson J, Fernando M, Clark L, Ince P, Matthews F, Forster G, O'Brien J, Barber R, Kalaria R, Brayne C. White matter lesions in an unselected cohort of the elderly: astrocytic, microglial and oligodendrocyte precursor cell responses. Neuropathol Appl Neurobiol 2007;33:410–9.

63. Lamar M, Zhou XJ, Charlton RA, Dean D, Little D, Deoni SC. In vivo quantification of white matter microstructure for use in aging: a focus on two emerging techniques. Am J Geriatr Psychiatry 2014;22:111–21.

64. Deoni SCL, Peters TM, Rutt BK. High-resolution T1 and T2 mapping of the brain in a clinically acceptable time with DESPOT1 and DESPOT2. Magn Reson Med 2005;53:237–41.

65. Pickering TG, Hall JE, Appel LJ, Falkner BE, Graves J, Hill MN, Jones DW, Kurtz T, Sheps SG, Roccella EJ. Recommendations for blood pressure measurement in humans and experimental animals part 1: blood pressure measurement in humans: a statement for

professionals from the Subcommittee of Professional and Public Education of the American Heart Association Council on High Blood Pressure Research. Hypertension 2005;45:142–61.

66. Eklund A, Nichols T, Knutsson H. Can parametric statistical methods be trusted for fMRI based group studies? ArXiv Prepr [Internet]. 2015; Available from: http://arxiv.org/abs/1511.01863

67. Dzau VJ, Antman EM, Black HR, Hayes DL, Manson JE, Plutzky J, Popma JJ, Stevenson W. The cardiovascular disease continuum validated: clinical evidence of improved patient outcomes part i: pathophysiology and clinical trial evidence (risk factors through stable coronary artery disease). Circulation 2006;114:2850–70.

Figure Legends

Figure 1. Cortical thickness associations between (A) BP and right lateral occipital; (B) Chol and left caudal medial frontal; (C) MetabDys and left inferior parietal; (D) MetabDys and left precuneus; (E) MetabDys and right superior parietal NOTE: Whole brain cortical thickness results derived from FreeSurfer. Maps were smoothed with a 15mm full width half maximum Gaussian kernel and correction for multiple comparisons was performed using the Monte Carlo Null-z simulation (p<0.05). All analyses have been adjusted for age and sex. Red indicates negative associations with cortical thickness and yellow indicates positive associations with cortical thickness.

Figure 2. TBSS results in red overlayed on the mean white matter tract skeleton (in green) derived from FSL using non-parametric permutation testing and cluster-based thresholding correction (p<0.001, cluster size>100 voxels). Significant cluster voxels associated with GluDys and fractional anisotropy adjusted for age and sex are depicted by the arrows pointing to the right inferior longitudinal fasciculus (ILF) and the right and left superior longitudinal fasciculus (SLF).

Table I: Sample characteristics

	Cognitive Sample (n=124)	Neuroimaging Sample (n=86)	p-value
DEMOGRAPHICS			
Age, years	59.8±13.1	61.7±12.6	0.31
Education, years	15.6±2.7	15.9±2.8	0.55
Sex (M:F)	62:62	43:43	0.56
Race (Caucasian:African American:Other)	62:51:11	51:28:7	0.69
MMSE	28.9±1.2	29.0±1.1	0.42
CARDIOVASCULAR RISK FACTORS			p-value
Systolic blood pressure, mmHg	132.4±15.2	133.1±13.7	0.64
Diastolic blood pressure, mmHg	79.6±9.5	80.3±10.0	0.61
Body mass index, kg/m^2	29.9±7.7	28.2±6.1	0.18
Total cholesterol, mg/dl	186.6±44.6	184.8±42.6	0.95
LDL cholesterol, mg/dl	103.2±39.1	99.2±34.9	0.62
HDL cholesterol, mg/dl	57.7±19.1	61.0±19.6	0.17
Triglycerides, mg/dl	128.2±67.0	122.3±64.9	0.52
Glucose, mg/dl	103.4±29.5	101.3±23.3	0.94
HbA1c, %	6.3±1.2	6.1±0.9	0.41

Note: All p>0.05. All values represent mean±standard deviation unless otherwise noted.

M:F=male:female, MMSE=Mini-Mental State Examination, HbA1c=hemoglobin A1c

Table II: Varimax rotated factor matrix from PCA

	Component 1	Component 2	Component 3	Component 4
Total Cholesterol	**0.990**	-0.049	-0.052	-0.042
LDL Cholesterol	**0.954**	0.030	0.045	0.075
Glucose	0.001	**0.902**	0.014	-0.121
Hemoglobin A1c	-0.063	**0.889**	0.239	0.080
Triglycerides	0.123	0.002	**0.828**	-0.140
HDL Cholesterol	-0.269	0.175	**0.794**	0.151
Body Mass Index	0.124	0.422	**0.521**	0.122
Systolic Blood Pressure	-0.046	-0.022	0.020	**0.854**
Diastolic Blood Pressure	0.075	0.008	0.019	**0.855**
Eigenvalue	2.367	1.982	1.544	1.125

Note: Minimum eigenvalue extraction=1.

Table III: Regression results for the association between cardiovascular risk factor and cognitive domains

	Learning β, SE, (p-value)	Memory β, SE, (p-value)	Executive Function β, SE, (p-value)	Attention/ Information Processing β, SE, (p-value)
Cholesterol	-0.008 0.071 (0.91)	0.046 0.068 (0.50)	0.011 0.057 (0.84)	0.031 0.070 (0.66)
Glucose	-0.088 0.075 (0.24)	-0.076 0.071 (0.29)	-0.114 0.060 (0.058)	-0.209 0.074 (0.006)*
Metabolic	-0.115 0.094 (0.22)	-0.116 0.090 (0.20)	0.017 0.075 (0.82)	0.089 0.093 (0.34)
Blood Pressure	-0.193 0.081 (0.019)*	-0.224 0.077 (0.005)*	-0.142 0.065 (0.031)*	-0.153 0.080 (0.060)

Note: *$p<0.050$, analyses were adjusted for age, education, and sex.

Table IV: Significant clusters of cortical thickness associated with cardiovascular risk factor
domain scores

	Region	Cluster Size (mm^2)	Max Z	X, Y, Z Talairach Coordinates
Cholesterol	Left Caudal Middle Frontal	1450.9	3.377	-38.3, 9.4, 49.3
Metabolic	Right Superior Parietal	7117.6	3.899	22.8, -40.9, 57.8
	Left Inferior Parietal	4817.1	3.222	-39.3, -70.0, 34.6
	Left Precuneus	1969.9	3.812	-6.8, -59.5, 41.8
Blood Pressure	Right Lateral Occipital	1699.7	-3.644	43.8, -77.8, -6.2

NOTE: Whole brain results adjusted for age and sex derived from Freesurfer. Maps were
smoothed with a 15mm FWHM Gaussian kernel and corrected for multiple comparisons using
the Monte Carlo Null-z simulation ($p < 0.050$).

Supplementary Table I: Multiple linear regression results for the association between cardiovascular risk factor component scores and cortical thickness regions of interest

	Cholesterol β, SE, (p-value)	Glucose β, SE, (p-value)	Metabolic β, SE, (p-value)	Blood Pressure β, SE, (p-value)
Caudal Anterior Cingulate L	-0.023, 0.017, (0.19)	0.000, 0.017, (0.99)	-0.014, 0.021, (0.50)	0.004, 0.020, (0.84)
R	-0.010, 0.016, (0.51)	0.001, 0.016, (0.96)	0.006, 0.019, (0.73)	-0.001, 0.018, (0.94)
Caudal Middle Frontal L	0.018, 0.006, (0.003)*	-0.010, 0.006, (0.12)	-0.005, 0.008, (0.47)	0.012, 0.007, (0.092)
R	0.005, 0.006, (0.39)	-0.009, 0.006, (0.11)	-0.004, 0.007, (0.59)	0.010, 0.006, (0.10)
Cuneus L	0.003, 0.006, (0.61)	0.000, 0.006, (0.98)	0.006, 0.007, (0.41)	0.003, 0.007, (0.67)
R	-0.001, 0.006. (0.90)	0.000, 0.006. (0.99)	0.002, 0.007, (0.83)	-0.003, 0.007, (0.65)
Entorhinal L	0.018, 0.018, (0.30)	-0.014, 0.018, (0.42)	0.001, 0.022, (0.95)	0.002, 0.020, (0.92)
R	-0.010, 0.022, (0.67)	0.002, 0.022, (0.94)	-0.038, 0.027, (0.16)	0.033, 0.025, (0.19)
Fusiform L	0.008, 0.006, (0.20)	-0.004, 0.006, (0.54)	-0.005, 0.008, (0.48)	0.001, 0.007, (0.87)
R	0.012, 0.007, (0.10)	-0.007, 0.007, (0.36)	-0.008, 0.009, (0.36)	-0.012, 0.008, (0.13)
Inferior Parietal L	0.000, 0.006, (0.97)	0.012. 0.005, (0.036)*	0.011, 0.007, (0.095)	-0.030, 0.006, (0.11)
R	0.007, 0.006, (0.22)	0.001, 0.006, (0.81)	-0.002, 0.007, (0.81)	-0.007, 0.007, (0.31)
Inferior Temporal L	0.010, 0.007, (0.15)	-0.007, 0.007, (0.30)	-0.014, 0.008, (0.076)	-0.006, 0.008, (0.43)
R	-0.003, 0.007, (0.67)	0.001, 0.007, (0.89)	-0.009, 0.009, (0.32)	-0.015, 0.008, (0.072)
Lateral Occipital L	0.006, 0.006, (0.29)	0.008, 0.006, (0.17)	0.005, 0.007, (0.50)	-0.006, 0.007, (0.40)
R	0.006, 0.006, (0.34)	0.007, 0.006, (0.27)	-0.006, 0.007, (0.42)	-0.041, 0.007, (0.041)*
Lateral Orbitofrontal L	0.008, 0.007, (0.28)	-0.011, 0.007, (0.14)	-0.036, 0.008, (<0.001)*	0.005, 0.008, (0.53)
R	0.000, 0.007, (0.99)	-0.009, 0.007, (0.24)	-0.016, 0.009, (0.068)	0.007, 0.008, (0.43)
Lingual L	0.001, 0.005, (0.82)	-0.005, 0.005, (0.34)	0.000, 0.006, (0.99)	-0.001, 0.006, (0.90)
R	0.004, 0.006, (0.53)	0.000, 0.006, (0.93)	-0.003, 0.007, (0.69)	0.005, 0.007, (0.48)
Medial Orbitofrontal L	0.003, 0.009, (0.78)	-0.007, 0.009, (0.46)	-0.025, 0.011, (0.023)*	0.000, 0.010, (0.99)
R	-0.009, 0.011, (0.42)	-0.016, 0.011, (0.16)	-0.035, 0.013, (0.007)*	-0.006, 0.012, (0.614)
Middle Temporal L	0.002, 0.006, (0.75)	-0.010, 0.006, (0.088)	-0.018, 0.007, (0.009)*	-0.012, 0.006, (0.068)
R	0.002, 0.006, (0.70)	-0.003, 0.006, (0.66)	-0.011, 0.008, (0.17)	-0.015, 0.007, (0.039)*
Parahippocampal L	0.025, 0.017, (0.14)	-0.023, 0.017, (0.17)	-0.032, 0.020, (0.12)	-0.024, 0.019, (0.21)
R	0.008, 0.015, (0.62)	-0.014, 0.015, (0.37)	-0.020, 0.019, (0.28)	-0.009, 0.017, (0.59)
Parsopercularis L	-0.001, 0.006, (0.86)	-0.012, 0.005, (0.029)*	-0.011, 0.007, (0.095)	0.001, 0.006, (0.93)
R	0.009, 0.006, (0.17)	-0.006, 0.006, (0.32)	-0.009, 0.008, (0.26)	-0.005, 0.007, (0.49)

Parsorbitalis L	-0.006, 0.010, (0.53)	-0.005, 0.010, (0.65)	-0.031, 0.012, (0.009)*	0.002, 0.011, (0.89)
R	-0.014, 0.009, (0.14)	0.002, 0.010, (0.87)	-0.007, 0.012, (0.55)	0.013, 0.011, (0.22)
Parstriangularis L	0.005, 0.007, (0.54)	-0.008, 0.007, (0.30)	-0.014, 0.009, (0.12)	0.009, 0.008, (0.30)
R	-0.002, 0.008, (0.80)	-0.012, 0.008, (0.13)	-0.014, 0.009, (0.14)	-0.003, 0.009, (0.72)
Posterior Cingulate L	0.007, 0.007, (0.32)	0.000, 0.007, (0.96)	0.002, 0.008, (0.80)	-0.006, 0.008, (0.41)
R	-0.001, 0.007, (0.88)	0.011, 0.007, (0.13)	0.005, 0.009, (0.60)	-0.009, 0.008, (0.29)
Precuneus L	0.004, 0.005, (0.48)	0.006, 0.005, (0.28)	0.011, 0.006, (0.078)	0.001, 0.006, (0.88)
R	0.006, 0.006, (0.27)	0.009, 0.006, (0.11)	0.003, 0.007, (0.70)	-0.004, 0.006. (0.54)
Rostral Anterior Cingulate L	0.006, 0.015, (0.71)	-0.013, 0.015, (0.40)	-0.020, 0.018, (0.27)	-0.005, 0.017, (0.77)
R	0.019, 0.014, (0.18)	-0.024, 0.014, (0.091)	-0.024, 0.017, (0.17)	-0.002, 0.016, (0.90)
Rostral Middle Frontal L	-0.002, 0.005, (0.66)	-0.003, 0.005, (0.60)	-0.008, 0.006, (0.22)	0.005, 0.006, (0.41)
R	-0.001, 0.005, (0.86)	-0.005, 0.005, (0.37)	-0.002, 0.006, (0.78)	0.007, 0.006, (0.21)
Superior Frontal L	0.003, 0.005, (0.59)	0.003, 0.005, (0.53)	0.006. 0.006, (0.37)	0.003, 0.006, (0.65)
R	0.010, 0.005, (0.053)	0.001, 0.005, (0.90)	0.002, 0.006, (0.70)	0.013, 0.006, (0.026)*
Superior Parietal L	0.006, 0.006, (0.35)	0.009, 0.006, (0.14)	0.014, 0.007, (0.061)	-0.004, 0.007, (0.60)
R	0.006, 0.006, (0.28)	0.008, 0.006, (0.16)	0.016, 0.007, (0.015)*	-0.001, 0.006, (0.93)
Superior Temporal L	0.004, 0.007, (0.59)	-0.011, (0.007), (0.12)	-0.006, 0.008, (0.49)	-0.015, 0.008, (0.061)
R	0.006, 0.007, (0.39)	-0.012, 0.007, (0.12)	-0.001, 0.009, (0.88)	-0.019, 0.008, (0.027)*

Note: L=left hemisphere, R=right hemisphere, *p<0.05, All analyses have been adjusted for age, sex

Supplementary Table II: Association between individual cardiovascular disease risk factor components and cortical thickness linear regression results where p was ≤0.050

a) Cholesterol Domain

	Total Cholesterol β, SE, (p-value)	LDL Cholesterol β, SE, (p-value)
L. Caudal Middle Frontal	0.002, 0.006, (0.001)*	0.015, 0.006, (0.013)*

Note: *p<0.05, All analyses have been adjusted for age, sex

b) Glucose domain

	Glucose β, SE, (p-value)	HbA1c β, SE, (p-value)
L. Inferior Parietal	0.011, 0.005, (0.033)*	0.009, 0.005, (0.090)
L. Parsopercularis	-0.010, 0.005, (0.045)*	-0.010, 0.005,(0.048)*

Note: *p<0.05, All analyses have been adjusted for age, sex

c) Metabolic domain

	Triglycerides β, SE, (p-value)	HDL Cholesterol β, SE, (p-value)	BMI β, SE, (p-value)
L. Lateral Orbitofrontal	-0.024, 0.006,(<0.001)*	0.026, 0.007,(<0.001)*	-0.016, 0.007, (0.014)*
L. Medial Orbitofrontal	-0.016, 0.008, (0.052)	0.025, 0.009, (0.007)*	-0.006, 0.008, (0.45)
R. Medial Orbitofrontal	-0.025, 0.010, (0.013)*	0.033, 0.011, (0.003)*	-0.009, 0.010, (0.37)
L. Middle Temporal	-0.009, 0.005, (0.090)	0.009, 0.006, (0.13)	-0.015, 0.005, (0.004)*
L. Parsorbitalis	-0.020, 0.009, (0.030)*	0.023, 0.010, (0.025)*	-0.015, 0.009, (0.098)
R. Superior Parietal	0.008, 0.005, (0.11)	-0.013, 0.006,(0.021)*	0.009, 0.005, (0.068)

Note: *p<0.05, All analyses have been adjusted for age, sex

d) Blood Pressure (BP) domain

	Systolic BP β, SE, (p-value)	Diastolic BP β, SE, (p-value)
R. Lateral Occipital	-0.014, 0.006, (0.017)*	-0.007, 0.006, (0.23)
R. Middle Temporal	-0.015, 0.006, (0.15)*	-0.008, 0.006, (0.23)
R. Superior Frontal	0.011, 0.005, (0.029)*	0.008, 0.005, (0.093)
R. Superior Temporal	-0.011, 0.007, (0.14)	-0.017, 0.007,(0.017)*

Note: *p<0.050, All analyses have been adjusted for age, sex

Supplementary Table III: Multiple linear regression results for the association between cardiovascular risk factor component scores and diffusion tensor imaging regions of interest

	Cholesterol β, SE, (p-value)	Glucose β, SE, (p-value)	Metabolic β, SE, (p-value)	Blood Pressure β, SE, (p-value)
Superior Longitudinal Fasciculus	0.002, 0.001, (0.013)*	-0.002, 0.001, (0.014)*	0.000, 0.001, (0.99)	0.000, 0.001, (0.99)
Superior Longitudinal Fasciculus Temporal	0.002, 0.001, (0.033)*	-0.003, 0.001, (0.013)*	0.000, 0.001, (0.82)	0.000, 0.001, (0.91)
Cingulum Hippocampus	0.001, 0.001, (0.37)	-0.002, 0.001, (0.17)	-0.002, 0.002, (0.16)	0.000, 0.001, (0.82)
Inferior Fronto-Occipital Fasciculus	0.002, 0.001, (0.089)	-0.003, 0.001, (0.007)*	0.000, 0.001, (0.92)	0.002, 0.001, (0.24)
Inferior Longitudinal Fasciculus	0.002, 0.001, (0.23)	-0.003, 0.001, (0.087)	0.000, 0.004, (0.97)	0.002, 0.002, (0.15)
Anterior Thalamic Radiation	0.001, 0.001. (0.45)	-0.001, 0.001, (0.16)	0.002, 0.001, (0.13)	0.001, 0.001, (0.15)
Uncinate Fasciculus	0.003, 0.002, (0.12)	-0.003, 0.002, (0.13)	-0.001, 0.002, (0.73)	-0.001, 0.002, (0.51)

Note: *p<0.05, All analyses have been adjusted for age, sex

-

Figure 1. Cortical thickness associations between (A) BP and right lateral occipital; (B) Chol and left caudal medial frontal; (C) MetabDys and left inferior parietal; (D) MetabDys and left precuneus; (E) MetabDys and right superior parietal NOTE: Whole brain cortical thickness results derived from FreeSurfer. Maps were smoothed with a 15mm full width half maximum Gaussian kernel and correction for multiple comparisons was performed using the Monte Carlo Null-z simulation (p<0.05). All analyses have been adjusted for age and sex. Red indicates negative associations with cortical thickness and yellow indicates positive associations with cortical thickness.
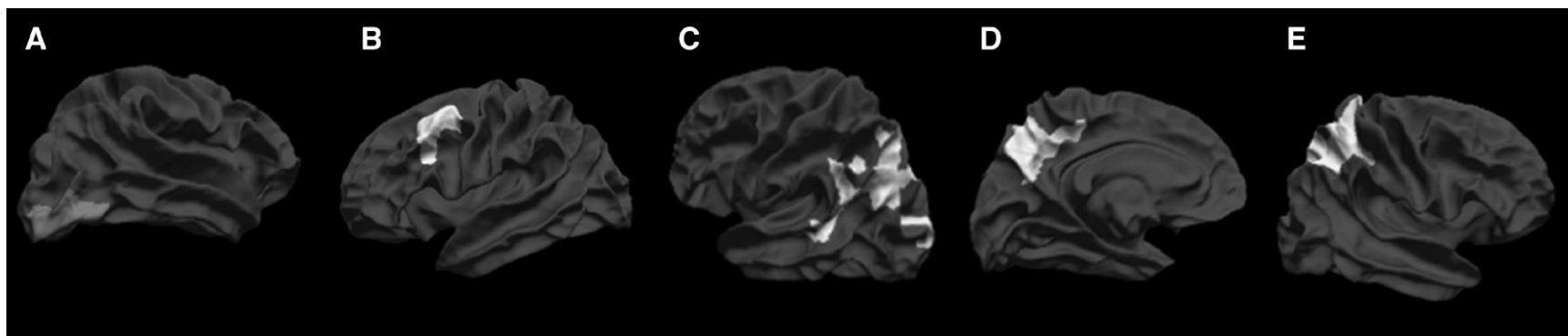
Figure 2. TBSS results in red overlayed on the mean white matter tract skeleton (in green) derived from FSL using non-parametric permutation testing and cluster-based thresholding correction (p<0.001, cluster size>100 voxels). Significant cluster voxels associated with GluDys and fractional anisotropy adjusted for age and sex are depicted by the arrows pointing to the right inferior longitudinal fasciculus (ILF) and the right and left superior longitudinal fasciculus (SLF).